



Modeling Sediment Transport Dynamics in Thompson Island Pool, Upper Hudson River

C. KIRK ZIEGLER

kziegler@qeallc.com

Quantitative Environmental Analysis, LLC, 305 West Grand Avenue, Montvale, NJ 07645

PETER H. ISRAELSSON

Quantitative Environmental Analysis, LLC, 305 West Grand Avenue, Montvale, NJ 07645

JOHN P. CONNOLLY

Quantitative Environmental Analysis, LLC, 305 West Grand Avenue, Montvale, NJ 07645

Abstract. Two-dimensional, vertically-averaged hydrodynamic and sediment transport models were developed and applied as part of a PCB fate and transport modeling study of Thompson Island Pool (TIP), Upper Hudson River. Mechanistic formulations were used to simulate cohesive and non-cohesive suspended load transport; site-specific data were extensively used to determine model inputs. This modeling approach is compared and contrasted to non-mechanistic solids transport sub-models used in other contaminant fate studies. A minimum number of model parameters were adjusted to calibrate the sediment transport model using data collected during the 1994 spring flood. The model was validated during the 1997 spring flood and for a 22-year (1977-1998) period. Successful calibration and validation of the model showed that: (1) deposition and resuspension processes were realistically and accurately formulated in the model; (2) the model is an effective diagnostic tool for quantitatively evaluating net deposition and erosion from various areas of TIP; and (3) sediment transport results can be coupled with a PCB fate model with a high degree of confidence.

Keywords: Sediment transport, modeling, Upper Hudson River

1. Introduction

Over an approximate 30-year period, ending in 1977, two General Electric (GE) capacitor manufacturing facilities in Fort Edward and Hudson Falls, New York discharged wastewater containing polychlorinated biphenyls (PCBs) into the Upper Hudson River (UHR). Much of the PCBs accumulated in the sediments upstream of the former Fort Edward Dam located approximately 3 km downstream of the Hudson Falls capacitor plant. Removal of this dam in 1973 and subsequent high flow events resulted in the movement of large quantities of PCB-containing sediments downstream. Some of these sediments deposited further downstream in pools formed by dams along the Champlain Canal, which is coincident with the UHR channel. Most of the historically-deposited, sediment-associated PCBs are now sequestered below the sediment surface, a consequence of the continual deposition of watershed-derived particulate matter. However, the contaminated bed sediments near or at the sediment surface are an "active" source of PCBs to the water column and to biota.

In 1990, the U.S. Environmental Protection Agency (USEPA) began a reassessment of the 1984 "No Action" decision for the sediments in the UHR. Recognizing the complexity and dynamic nature of the links between the sediment PCB levels and PCB levels in the

water column and biota, GE undertook the development of a mass balance model. The purpose of the model is to provide scientifically reliable estimates of future PCB levels within the river. The model framework consists of four sub-models: hydrodynamic; sediment transport; PCB fate and transport; and PCB bioaccumulation. The hydrodynamic and sediment transport models will be the focus of this paper. A complete description of the modeling framework is presented in QEA (1999); an on-line copy of this report is located at www.hudsonwatch.com. The PCB fate model is described in Connolly et al. (2000).

Sediment transport processes are controlling factors in the fate and transport of PCBs in the UHR. Natural recovery in the river is primarily controlled by sedimentation, which is affected by resuspension and deposition processes, as well as sediment loading. Bed erosion during a rare flood event, e.g., 100-year flood, which could possibly cause elevated bed PCB concentrations buried at depth to be introduced back into the bioavailable zone, is determined by hydrodynamic processes and properties of the sediment bed. Thus, understanding and quantifying sediment transport processes is of critical importance when evaluating PCB fate in the river and the effectiveness of various remedial alternatives.

Many previous contaminant fate and transport modeling studies have used solids transport sub-models that are relatively simplistic, non-mechanistic, empirical and poorly constrained. This type of model has generally produced unsatisfactory results, largely because of inadequacies in the sediment transport sub-model. In the study described in this paper, a mechanistic sediment transport model has been applied to the UHR, with sediment transport results being transferred to a PCB fate model (Connolly et al., 2000). One objective of this paper is to provide a description of the development, calibration and validation of the hydrodynamic and sediment transport sub-models in order to demonstrate the scientific credibility of the model. Two additional goals of this paper are: 1) provide a discussion of data analyses and modeling techniques that are used to develop and apply a relatively sophisticated, mechanistic sediment transport model; and 2) contrast the current effort with previous studies that have used non-mechanistic approaches. This discussion will hopefully aid other modelers that are using contaminant fate models and make it possible to improve the predictive capability and reliability of future models.

2. Description of Study Area

The UHR is a run-of-the-river reservoir system, comprised of a series of eight dams and associated backwaters, which extends from Fort Edward to Troy, New York, a distance of approximately 64 km. Hydrodynamic and sediment transport models have been developed, calibrated and validated for each of the eight reaches in the UHR (QEA, 1999). This paper describes the hydrodynamic and sediment transport models developed for Thompson Island Pool (TIP), which is the first reach downstream of Fort Edward. TIP is the pool immediately downstream of Fort Edward, and it has a length of 9.6 km. This reach of the UHR is the region of principal focus of the USEPA reassessment because the highest UHR PCB concentrations, in the bed and biota, are found in TIP. In addition, comprehensive data sets, spanning more than 20 years, are available for this reach, making it possible to adequately calibrate and validate all four sub-models.

TIP extends from Fort Edward to its termination at Thompson Island Dam, which is an uncontrolled, low-head dam that is 1.2 m high (Figure 1). The average width of TIP is 210 m and this reach has a surface area of 200 ha. The mean water depth in this reach is about 3 m, with significant lateral variability in depth due to the Champlain Canal navigational channel. The central channel of the river, which has been dredged in the past, has maximum depths of 6-7 m. Shallower, nearshore areas typically have depths of 1-2 m. Generally, the sediment bed in the deeper central channel areas is primarily composed of sand, gravel and rock; cohesive sediment deposits are usually located in the shallower, nearshore areas.

The mean flow rate of the UHR at Fort Edward is 147 m³/s, with the average flow rate at the dam higher than this by about 6 m³/s. The flow increase is due to tributary and direct drainage flow into TIP from a 417 km² drainage basin. Approximately 80% of the total runoff comes from two primary tributaries (Snook Kill and Moses Kill), with the balance of the runoff from smaller creeks and direct runoff.

3. Hydrodynamic Model

Inclusion of this sub-model in any contaminant fate model is important because of the dependence of sediment resuspension and deposition on bottom shear stress, which is calculated by the hydrodynamic model. Typically, hydrodynamic models have not been coupled to contaminant fate models; past contaminant fate models have generally relied on simple flow routing techniques and have not calculated bottom shear stress (e.g., O'Connor et al., 1983; Velleux and Endicott, 1994). This simplistic representation of hydrodynamic processes should not be used. A hydrodynamic model is required in order to adequately simulate temporal and spatial variations in current velocity, water depth and bottom shear stress. The level of complexity that is needed, i.e., a one-, two- or three-dimensional hydrodynamic model, will depend on the geometry and flow conditions in a particular aquatic system and the degree of accuracy required for the study.

TIP is relatively shallow and its flow is unstratified. These conditions make it reasonable to assume that the water column is vertically well-mixed. Thus, the two-dimensional, vertically-averaged equations are an accurate approximation to the general three-dimensional equations of motion for an incompressible fluid. The conservation of mass and momentum equations applied to TIP are (Ziegler and Nisbet, 1994)

$$\frac{\partial \eta}{\partial t} + \frac{\partial(uh)}{\partial x} + \frac{\partial(vh)}{\partial y} = 0 \quad (1)$$

$$\begin{aligned} \frac{\partial(uh)}{\partial t} + \frac{\partial(u^2h)}{\partial x} + \frac{\partial(uvh)}{\partial y} = & -gh \frac{\partial \eta}{\partial x} - C_f qu + \frac{\partial}{\partial x} \left(hB_H \frac{\partial u}{\partial x} \right) \\ & + \frac{\partial}{\partial y} \left(hB_H \frac{\partial u}{\partial y} \right) \end{aligned} \quad (2)$$

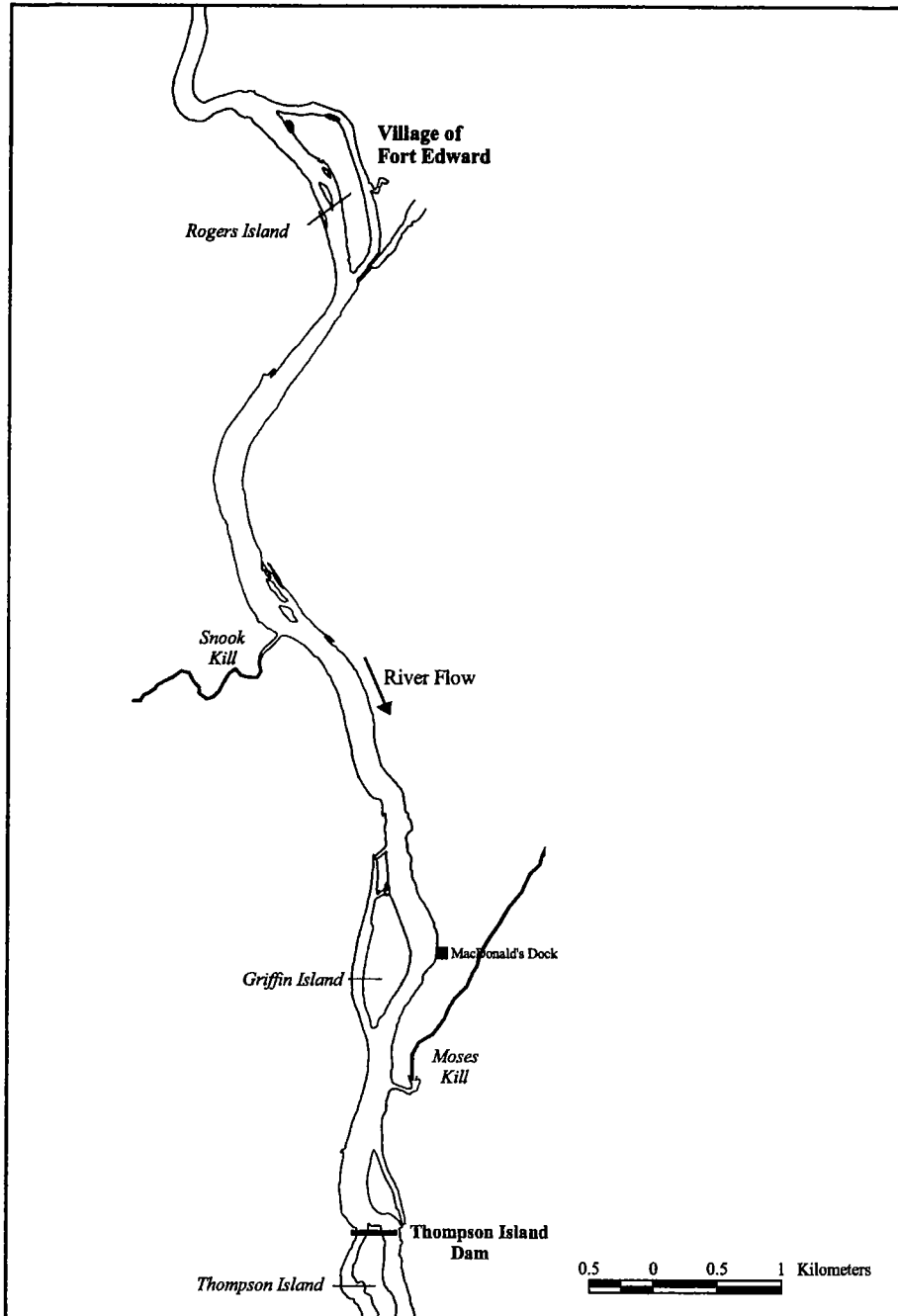


Figure 1. Thompson Island Pool, Upper Hudson River.

$$\frac{\partial(vh)}{\partial t} + \frac{\partial(uvh)}{\partial x} + \frac{\partial(v^2h)}{\partial y} = -gh \frac{\partial\eta}{\partial y} - C_f qv + \frac{\partial}{\partial x} \left(hB_H \frac{\partial v}{\partial x} \right) + \frac{\partial}{\partial y} \left(hB_H \frac{\partial v}{\partial y} \right) \quad (3)$$

where the total water depth is $h = h_o + \eta$; h_o = reference water depth; η = water surface displacement with respect to reference depth; u, v = velocities along the x- and y-axes, respectively; $q = (u^2 + v^2)^{1/2}$; C_f = spatially variable bottom friction factor; and B_H = horizontal eddy viscosity. Note that the x-axis is oriented in the longitudinal (along-channel) direction and the y-axis is oriented in the lateral (cross-channel) direction. Equations (1) to (3) were transformed from Cartesian coordinates to orthogonal, curvilinear coordinates in order to resolve more accurately the complex geometry and bathymetry of TIP. The resulting equations were solved numerically using the semi-implicit version of a well-established hydrodynamic model, ECOM (Blumberg, 1994).

The bottom friction factor in Equations (2) and (3) is dependent on the local water depth and effective bottom roughness (Blumberg and Mellor, 1983)

$$C_f = \text{MAX} \left[\frac{\kappa^2}{\left(\ln \frac{h}{z_o} \right)^2}, C_{f,\text{min}} \right] \quad (4)$$

where κ = von Karman's constant (0.4); $C_{f,\text{min}}$ = minimum bottom friction factor; and z_o = effective bottom roughness. The bottom friction factor (C_f) thus varies both spatially and temporally due to changes in total water depth (h) and bottom roughness (z_o). Spatial variations in bottom roughness are included by using different z_o values for cohesive and non-cohesive sediment bed types. It was assumed that bottom roughness in non-cohesive and hard bottom areas (which used the same z_o value) is greater than z_o in cohesive bed areas, which is consistent with the physical characteristics of those two bed types. Cohesive beds are hydraulically smoother than non-cohesive beds because: (1) median sediment particle diameter (d_{50}) is lower and (2) bed forms tend to be absent or significantly smaller.

The model extends from Route 197 bridge at Rogers Island to Thompson Island Dam. This reach was discretized using 68 longitudinal and 10 lateral grid cells (QEA, 1999). Average longitudinal grid cell size was 140 m and typical lateral grid cell size was about 20-30 m. Bathymetric data collected in TIP in 1991 were used to specify values of h_o for model input (O'Brien and Gere, 1993). The 1991 bathymetric survey collected depth soundings at about 107,000 points throughout TIP at river flows that ranged from about 48 to 76 m³/s. The reference water depth (h_o) in each grid cell was calculated by averaging the 1991 sounding data located within that grid cell.

The hydrodynamic model required specification of two types of time-variable boundary conditions: (1) inflows from upstream and tributary sources and (2) stage height at the

dam. Flow rates measured by the U.S. Geological Survey (USGS) at the Fort Edward gauging station were used as input at the upstream boundary of the model. Estimation of tributary discharge to TIP from Snook Kill, Moses Kill and direct runoff was accomplished using a modified drainage area proration method (QEA, 1999). Stage heights measured by Champlain Canal personnel in TIP (T. Rathwell, NYS Thruway Authority, *personal communication* 1996) were used to develop a relationship between flow rate and water surface elevation at the dam. The dam rating curve developed from these data was used to specify the time-variable downstream boundary condition (stage height at Thompson Island Dam) in all simulations.

4. Sediment Transport Model

Generally, relatively simplistic representations of resuspension and deposition processes have been used in past solids transport sub-models associated with contaminant fate models (e.g., O'Connor et al., 1983; Thomann et al., 1993; Velleux and Endicott, 1994). This approach uses non-mechanistic, empirical formulations to simulate resuspension and deposition fluxes at the sediment-water interface, i.e., resuspension and deposition velocities are treated as calibration parameters that can be adjusted temporally and/or spatially. Results from this type of model are typically unsatisfactory and yield predictions that are of questionable value because the sediment dynamics are not accurately and realistically formulated. More sophisticated, mechanistic sediment transport models have been developed and these types of models should be used; contaminant fate models using non-mechanistic solids transport formulations should not be applied in the future.

The sediment transport model used in the present study is a modified version of the SEDZL sediment transport model originally developed by Ziegler and Lick (1986). SEDZL has been used in a number of sediment transport studies, including Fox River in Wisconsin (Gailani et al., 1991), Pawtuxet River in Rhode Island (Ziegler and Nisbet, 1994), Lake Erie (Lick et al., 1994), Saginaw River in Michigan (Cardenas et al., 1995), Buffalo River in New York (Gailani et al., 1996) and Watts Bar Reservoir in Tennessee (Ziegler and Nisbet, 1995).

Suspended sediment particles in a river have a large range of sizes, from less than 1 μm clays to medium sands on the order of 400 μm . Simulation of the entire particle size spectrum is impractical. Therefore, particles were broadly segregated into two groups: silt and clay that may interact and form flocs and sand that is transported as discrete particles. The model uses this approach to approximate the particle size spectrum. "Class 1" particles include all the cohesive particles, i.e., clays and silts, with disaggregated particle diameters of less than 62 μm , while the "class 2" particles include coarser, non-cohesive sediments, primarily fine and medium sand with diameters between 62 and 425 μm . In the past, many contaminant fate models have only used one sediment size class, an approximation that may not produce realistic results. Significant temporal and spatial variations in suspended sediment composition can occur in a river (and do occur in TIP), making it necessary to use at least two sediment size classes.

A two-dimensional, vertically-averaged sediment transport equation for size-class k ($k = 1, 2$) was applied (Ziegler and Nisbet, 1994)

$$\frac{\partial(hC_k)}{\partial t} + \frac{\partial(uhC_k)}{\partial x} + \frac{\partial(vhC_k)}{\partial y} = \frac{\partial}{\partial x} \left(hE_x \frac{\partial C_k}{\partial x} \right) + \frac{\partial}{\partial y} \left(hE_y \frac{\partial C_k}{\partial y} \right) + R_k - D_k \quad (5)$$

where C_k = concentration of suspended sediment of size-class k ; E_x, E_y = horizontal eddy diffusivities along the x - and y -axes, respectively; R_k = resuspension (erosion) flux of size-class k ; and D_k = deposition flux of size-class k . Results from the hydrodynamic model provide information about the transport field in Equation (5), i.e., u, v and h . Similar to the hydrodynamic equations, Equation (5) has been transformed into an orthogonal, curvilinear coordinate system and solved numerically. The hydrodynamic and sediment transport models used the same numerical grids.

5. Deposition Processes

As mentioned above, cohesive sediments in the water column range from clay particles smaller than $1 \mu\text{m}$ up to $\sim 62 \mu\text{m}$ silts. The discrete particles aggregate and form flocs that can vary greatly in size and effective density. Variations in concentration and shear stress affect both floc diameter and settling speed (Burban et al., 1990). Previous modeling studies (Ziegler and Nisbet, 1994, 1995; Gailani et al., 1996) have shown that an effective approximation is to treat suspended cohesive sediments as a single class. This approach assumes that the settling and depositional characteristics of cohesive sediments can be represented by average values of a distribution of properties. Using this approximation, the deposition flux of cohesive (class 1) sediments to the sediment bed is expressed as (Ziegler and Nisbet, 1994)

$$D_1 = P_1 W_{s,1} C_1 \quad (6)$$

where $W_{s,1}$ = cohesive sediment settling speed and P_1 = probability of deposition for cohesive sediments.

Settling speeds of cohesive flocs have been measured over a large range of concentrations and shear stresses in freshwater (Burban et al., 1990). The Burban settling speed data for cohesive flocs in freshwater were analyzed to develop a formulation to approximate the effects of flocculation on settling speed. This analysis indicated that the settling speed is dependent on the product of the concentration (C_1) and the water column shear stress (G) at which the flocs are formed, resulting in the following relationship

$$W_{s,1} = 2.5(C_1 G)^{0.12} \quad (7)$$

where the units of $W_{s,1}$, C_1 , and G are m/day , mg/l and Pa , respectively (Figure 2). For a depth-averaged model, as used in this study, the relevant shear stress for use in Equation

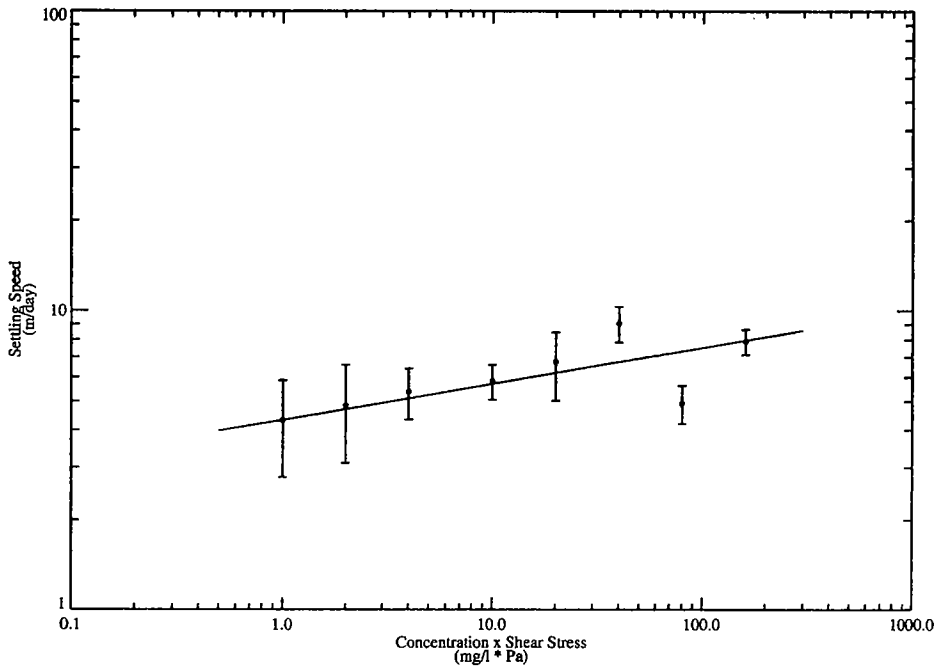


Figure 2. Settling speed function for cohesive (class 1) sediment (solid line) and floc settling speed data (mean \pm 95% confidence interval, Burban et al., 1990) used to construct function.

(7) is the bottom shear stress (τ_b), i.e., $G = \tau_b = \rho_w C_f q^2$ and $\rho_w =$ water density (assumed to be $1,000 \text{ kg/m}^3$). A previous analysis of the Burban data by Ziegler (Gailani et al., 1991) produced different settling speed formulations than Equation (7). A review of the earlier formulations showed that those equations do not accurately represent the Burban settling speed data. Hence, the present formulation, Equation (7), should be used instead of the equations originally developed by Ziegler (Gailani et al., 1991; Ziegler and Nisbet, 1994, 1995).

Modeling suspended cohesive sediments as a single class, with an effective $W_{s,1}$ given by Equation (7), makes it necessary to use a probability of deposition (P_1) to parameterize the effects of particle/floc size heterogeneity and near-bed turbulence on the deposition rate. The complex interactions occurring in the vicinity of the sediment-water interface cause only a certain fraction of the settling cohesive sediments, represented by P_1 , to become incorporated into the bed (Krone, 1962; Partheniades, 1992). An experimentally-based formulation that represents the effects of variable floc size on probability of deposition was developed by Partheniades (1992) (Figure 3)

$$P_1 = 1 - (2\pi)^{-1/2} \int_{-\infty}^Y e^{-\frac{w^2}{2}} dw \quad (8)$$

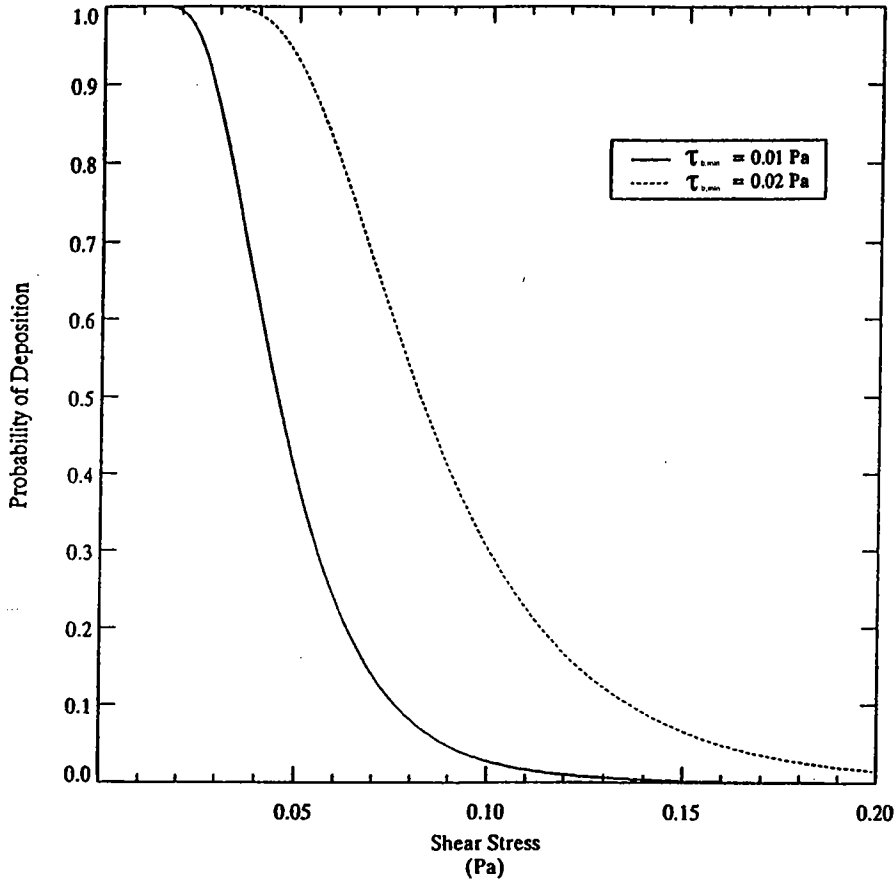


Figure 3. Probability of deposition function for cohesive (class 1) sediment.

where

$$Y = 2.04 \ln \left[0.25 \left(\frac{\tau_b}{\tau_{b,\min}} - 1 \right) e^{1.27 \tau_{b,\min}} \right] \quad (9)$$

and $\tau_{b,\min}$ = bottom shear stress below which $P_1 = 1$. A value of 0.01 Pa was used for $\tau_{b,\min}$ and not adjusted during model calibration. This value is consistent with $\tau_{b,\min}$ values reported by Partheniades (1992). Non-mechanistic solids transport sub-models have used a constant effective settling speed (O'Connor et al., 1983; Velleux and Endicott, 1994), an approximation which neglects the important effects of near-bed turbulence on deposition and can produce unrealistic results because significant temporal and spatial variations in τ_b and P_1 occur in any river.

Class 2 particles, i.e., fine and medium sand, suspended in the water column have an effective settling speed ($W_{s,2}$) that depends on the effective particle diameter (d_2). The relationship between $W_{s,2}$ and d_2 was developed by Cheng (1997). The depositional flux for this sediment class is estimated as

$$D_2 = P_2 W_{s,2} \Gamma C_2 \quad (10)$$

where P_2 = probability of deposition for non-cohesive sediments and Γ = class 2 stratification correction factor. Details concerning methods for calculating Γ , $W_{s,2}$ and P_2 are presented in Appendix B. Significant vertical stratification of class 2 sediment can occur in the water column due to the high settling speeds of fine and medium sand. This characteristic means that accurate calculation of class 2 deposition flux requires use of the near-bed concentration ($C_{a,2}$), where $C_{a,2} = \Gamma C_2$ and $\Gamma > 1$. Note that Γ is dependent upon $W_{s,2}$, τ_b , bottom roughness and local depth.

Examination of Equations (6) and (10) shows that the “effective” settling speed of class 1 ($P_1 W_{s,1}$) is typically one to two orders of magnitude lower than that of class 2 ($P_2 W_{s,2} \Gamma$). This differential has significant impact on simulation results and underscores the importance of using two sediment size classes as opposed to a single size class as has been typically used in many contaminant fate models.

6. Cohesive Resuspension Processes

Experimental results have shown that a finite amount of material will typically be resuspended from a fine-grained, cohesive sediment bed exposed to a constant bottom shear stress. This phenomenon, referred to as bed armoring, has been observed and quantified in a number of laboratory (Parchure and Mehta, 1985; Tsai and Lick, 1987; Graham et al., 1992) and field studies (Hawley, 1991; Amos et al., 1992). The amount of fine-grained sediment resuspended from a cohesive deposit is (Gailani et al., 1991)

$$\epsilon = \frac{a_o}{T_d^N} \left(\frac{\tau_b - \tau_{cr}}{\tau_{cr}} \right)^n, \tau_b \geq \tau_{cr} \quad (11)$$

where ϵ = net mass of resuspended sediment per unit surface area (resuspension potential); a_o = site-specific constant; T_d = time after deposition in days; N , n = exponents dependent upon the deposition environment; and τ_{cr} = effective critical shear stress. Many contaminant fate models have used a resuspension velocity that is empirically determined during model calibration (O'Connor et al., 1983; Velleux and Endicott, 1994). This procedure can produce highly inaccurate results because: 1) site-specific data are not used to determine erosion parameters (and thus constrain the resuspension process); 2) bed consolidation effects are neglected; and 3) bed armoring effects are not simulated.

Experimental results show that cohesive erosion, for a bed exposed to a constant bottom shear stress, occurs over a time period on the order of one hour, i.e., ϵ mg/cm²

of sediment are eroded in about one hour (Tsai and Lick, 1987; MacIntyre et al., 1990). Thus, the total resuspension rate ($R_{tot,coh}$) is approximated by

$$R_{tot,coh} = \frac{\epsilon}{3600} \quad (12)$$

where $R_{tot,coh}$ is assumed to be constant until all available sediment is eroded. Once the amount ϵ has been resuspended, $R_{tot,coh}$ is set to zero until additional sediment is deposited and available for resuspension or until the shear stress increases (Gailani et al., 1991). The resuspension rate of class k (R_k) sediment from the cohesive bed is

$$R_k = f_k R_{tot,coh} \quad (13)$$

where f_k = fraction of class k sediment in the surficial layer of the cohesive bed. The present study models two classes of suspendable sediment, with f_1 corresponding to the fraction of cohesive particles (clay and silt) in the bed and f_2 representing the fraction of suspendable non-cohesive particles (fine and medium sand with particle diameters between 62 and 425 μm). The total fraction of suspendable sediment in the bed ($f_{sus} = f_1 + f_2$) is equal to one in the cohesive bed. In non-cohesive bed areas, f_{sus} can be less than or equal to one, depending on local conditions.

The effects of bed consolidation with depth and horizontal variations in bed composition are simulated using a three-dimensional model of the cohesive sediment bed. The layered bed model conserves mass, with mass flux occurring only at the sediment-water interface due to deposition and resuspension. Vertical variations of sediment bed consolidation, or equivalently porosity, are accounted for by discretizing the bed into seven layers. The time after deposition of the layers increases linearly from one day at the surface, which is composed of freshly deposited sediment, to seven days in the bottom layer. Previous laboratory studies (Tsai and Lick, 1987; MacIntyre et al., 1990) indicate that consolidation effects on resuspension are minimal after about seven days of consolidation. Therefore, the maximum age of deposited sediments was set at seven days. Consolidation effects on resuspension are accounted for in Equation (11) by the $(T_d)^{-N}$ term, which causes the resuspension potential (ϵ) to decrease as the bed consolidates with time. The critical shear stress, τ_{cr} , was assumed to be constant in all layers of the bed. The model accounts for changes in bed composition, i.e., f_1 and f_2 , due to resuspension and deposition during the course of a simulation.

7. Non-Cohesive Resuspension Processes

Simulation of non-cohesive resuspension in TIP is necessary because: 1) non-cohesive bed areas, composed primarily of sand and gravel, represent over 75% of the TIP sediment bed and 2) cohesive and non-cohesive resuspension processes are very different. Typically, non-mechanistic solids transport sub-models have not accounted

